

hca: an Arabidopsis mutant exhibiting unusual cambial activity and altered vascular patterning

Christophe Pineau¹, Amandine Freyrier¹, Philippe Ranocha¹, Alain Jauneau¹, Simon Turner², Gaëtan Lemonnier³, Jean-Pierre Renou³, Petr Tarkowski^{4,†}, Göran Sandberg⁴, Lise Jouanin⁵, Björn Sundberg⁴, Alain-Michel Boudet¹, Deborah Goffner¹ and Magalie Pichon^{1,*}

¹Surfaces Cellulaires et Signalisation chez les Végétaux, Unité Mixte de Recherche, Centre National de la Recherche Scientifique – Université Paul Sabatier 5546, Pôle de Biotechnologie Végétale, 24 Chemin de Borde Rouge, 31326 Castanet Tolosan, France,

²School of Biological Sciences, The University of Manchester, 3.614 Stopford Building, Oxford Road, Manchester M13 9PT, UK,

³INRA/CNRS – URGV 2, rue Gaston Crémieux, CP5708, 91057 Evry Cedex, France,

⁴Department of Forest Genetics and Plant Physiology, Umeå Plant Science Center, SLU, SE-901 83 Umeå, Sweden, and

⁵Laboratoire de Biologie Cellulaire, INRA, 78026 Versailles Cedex, France

Received 14 April 2005; revised 16 June 2005; accepted 22 July 2005.

*For correspondence (fax +33 562 193 502; e-mail pichon@scsv.ups-tlse.fr).

†Present address: Laboratory of Growth Regulators, Palacky University and Institute of Experimental Botany ASCR, Slechtitelu 11, 783 71, Olomouc, Czech Republic.

Summary

By screening a T-DNA population of Arabidopsis mutants for alterations in inflorescence stem vasculature, we have isolated a mutant with a dramatic increase in vascular tissue development, characterized by a continuous ring of xylem/phloem. This phenotype is the consequence of premature and numerous cambial cell divisions in both the fascicular and interfascicular regions that result in the loss of the alternate vascular bundle/fiber organization typically observed in Arabidopsis stems. The mutant was therefore designated high cambial activity (*hca*). The *hca* mutation also resulted in pleiotropic effects including stunting and a delay in developmental events such as flowering and senescence. The physiological characterization of *hca* seedlings *in vitro* revealed an altered auxin and cytokinin response and, most strikingly, an enhanced sensitivity to cytokinin. These results were substantiated by comparative microarray analysis between *hca* and wild-type plants. The genetic analysis of *hca* indicated that the mutant phenotype was not tagged by the T-DNA and that the *hca* mutation segregated as a single recessive locus, mapping to the long arm of chromosome 4. We propose that *hca* is involved in mechanisms controlling the arrangement of vascular bundles throughout the plant by regulating the auxin–cytokinin sensitivity of vascular cambial cells. Thus, the *hca* mutant is a useful model for examining the genetic and hormonal control of cambial growth and differentiation.

Keywords: *Arabidopsis thaliana*, cambium, secondary xylem, cytokinin hypersensitivity, vascular patterning, Complete Arabidopsis Transcriptome MicroArray (CATMA).

Introduction

Vascular tissues in plants are either primary or secondary. Primary xylem and phloem differentiate within the vascular cylinder during primary growth of stems and roots. Later in development, when elongation ceases and plants undergo secondary growth, a vascular cambium develops that gives rise to secondary xylem and secondary phloem (Esau, 1965). The dividing cambial initials produce phloem or xylem mother cells which subsequently undergo one or several rounds of division before differentiation. The ‘cambial zone’ includes the cambial initials and phloem

and xylem mother cells (Lachaud *et al.*, 1999; Larson, 1994). During both primary and secondary growth, positional information is necessary to coordinate the spatio-temporal formation of vascular strands not only throughout the plant organ but also within vascular bundles. Our current knowledge concerning the molecular mechanisms underlying many aspects of vascular development, such as control of cambial cell division, primary and secondary xylem/phloem differentiation and patterning, is still fragmented.

It is well known that plant hormones, and in particular auxin, play a crucial role in the developmental control of primary and secondary vascular tissues and cambial activity (Little and Pharis, 1995; Ye, 2002) by regulating both radial (Sundberg *et al.*, 2001; Uggla *et al.*, 1996) and longitudinal vascular pattern formation in plants (Berleth *et al.*, 2000; Sieburth, 1999). Developing buds and young shoots are major sources of auxin, but indole acetic acid (IAA) is also synthesized in young root tissues (Ljung *et al.*, 2002). Auxin is transported through the plant in a basipetal polar fashion (for reviews see Lomax *et al.*, 1995; Swarup and Bennett, 2003). In the canalization hypothesis proposed by Sachs (1981) this polar auxin transport has been related to the differentiation of provascular strands. In recent years, genetic studies of Arabidopsis mutants altered in auxin metabolism have increased our understanding of auxin transport and signal transduction in relation to vascular differentiation and patterning (for reviews see Berleth and Mattsson, 2000; Berleth *et al.*, 2000; Hobbie, 1998). It is known that polar auxin transport is mediated to a great extent by the efflux carrier PIN1. Based on the *pin1* mutant phenotype, it was also demonstrated that auxin transport has a central role in the formation of vascular strands (Gälweiler *et al.*, 1998). Many proteins involved in responses to auxin have been characterized, and at least two of them, PINOID, a putative protein kinase, and MP, an auxin response factor, have been shown to be important for vascular differentiation and patterning (Christensen *et al.*, 2000; Hardtke and Berleth, 1998).

Although there is some evidence pointing to a role for cytokinin in procambial cell division and xylem differentiation, its mode of action is not well understood (Saks *et al.*, 1984; for review see Aloni, 1995). *In vitro* studies of xylogenesis in *Zinnia elegans* indicate that auxin alone is not sufficient to induce the differentiation of leaf mesophyll cells into tracheary elements (TE), and that cytokinin is a strict requirement for differentiation of TE (Fukuda and Komamine, 1980). More recently, the characterization of the *wooden leg* (*wol*) mutant and the subsequent cloning of the corresponding gene, *CYTOKININ RESPONSE (CRE1)*, demonstrated that cytokinin regulates vascular development by controlling procambial cell division (Inoue *et al.*, 2001; Mähönen *et al.*, 2000). As a result of defective procambial cell divisions, all procambial cells in roots differentiate uniquely into protoxylem, with neither protophloem nor metaxylem forming in the stele. The *WOL/CRE1* gene encodes a cytokinin receptor which belongs to the two-component signal transducer family. It is expressed in procambial cells of primary roots.

Although we are still a long way from establishing an integrated model that thoroughly explains the differentiation of cambial cells into functional vascular bundles, important headway has been made in dissecting certain steps of vascular differentiation and patterning *per se* by

carrying out mutant screening for vascular defects. Many mutants with a variety of phenotypes have been characterized (for reviews see Fukuda, 2004; Scarpella and Meijer, 2004; Turner and Sieburth, 2002). In some cases, mutant analysis has resulted in a more precise function for some genes already known to be involved in secondary cell deposition. This is the case for *irx3* encoding cellulose synthase (Taylor *et al.*, 1999) and *irx4* encoding cinnamoyl Co-A reductase (Jones *et al.*, 2001). In other cases, genetic analysis has revealed the role of important regulatory genes in vascular formation. Recently, a MYB transcription factor, *ALTERED PHLOEM DEVELOPMENT (APL)* has been identified as a key player in phloem development (Bonke *et al.*, 2003). Another regulatory gene *INTERFASCICULAR FIBERLESS1 (IFL1)*, belonging to the homeodomain-leucine zipper protein (HD-ZIP) is essential for proper fiber differentiation in Arabidopsis stems (Ratcliffe *et al.*, 2000; Zhong and Ye, 1999; Zhong *et al.*, 1997). Although numerous vascular mutants have been described, to our knowledge mutants with altered cambial activity and/or secondary growth are extremely rare (Oyama *et al.*, 1997).

Contrary to preconceived notions, Arabidopsis is considered to be an excellent model for the study of secondary growth (Chaffey *et al.*, 2002). Under normal growth conditions, hypocotyls of mature plants possess a vascular cambium and undergo extensive secondary growth (Busse and Evert, 1999; Ye *et al.*, 2002). Secondary growth has also been described in the inflorescence stem (Altamura *et al.*, 2001), and this phenomenon is enhanced when plants are grown at a low population density and/or with repeated removal of all newly emerging inflorescences stems. Taking advantage of this characteristic, Zhao *et al.* (2000) constructed a cDNA library from root-hypocotyl sections enriched in developing xylem cells. Moreover, genes related to secondary growth were identified by hybridizing the Arabidopsis Genome GeneChip arrays with cDNA extracted from stems with enhanced secondary xylem formation (Ko *et al.*, 2004; Oh *et al.*, 2003).

Since Arabidopsis possesses a vascular cambium and undergoes secondary growth it should be possible to identify molecular and physiological factors that control cambial activity by identifying mutants altered in amounts or patterns of secondary vascular tissues. An assumption may be made that these alterations would be the direct consequence of altered cambial activity. To address this issue, we have screened a T-DNA collection of Arabidopsis and isolated a mutant that has abnormally high secondary xylem production in stems. In *hca* (for 'high cambial activity'), the extensive secondary growth altered the organization of the stem vasculature leading to a continuous ring of vascular tissues; the mutant is impaired in cambial activity and secondary growth throughout the plant body. We have demonstrated by multiple, independent assays that

responses to both auxin and cytokinin were affected in the *hca* mutant.

Results

Isolation of hca mutant with unusually high cambial activity

To dissect the molecular determinants that control vascular differentiation in plants, we screened an Arabidopsis T-DNA mutant collection (Beschold *et al.*, 1993) for altered vasculature. The basal portion of inflorescence stems from 6-week-old plants were systematically sectioned freehand and observed using light and UV fluorescence microscopy. This screening procedure allowed us to isolate a mutant line with a dramatically altered organization of vascular tissues. The vascular system of wild-type Arabidopsis is classically organized in discrete collateral bundles with the xylem towards the inside and the phloem towards the outside of the bundle. Vascular bundles are separated from each other by lignified interfascicular fibers (Figure 1a–c). In contrast, the mutant line exhibited a continuous ring of vascular tissues (Figure 1d–f) and was characterized by a loss of the alternate vascular bundle/fiber organization. Sclerenchyma fibers appeared as small aggregates irregularly dispersed within the numerous xylem files (data not shown). This phenotype suggested an atypically active cambium and was therefore designated *hca* for high cambial activity.

To investigate the altered vasculature of *hca* in more detail, thin sections from the base of the stem were observed (Figure 1g–j). In the wild type (Figure 1i), the vascular bundles and the interfascicular fibers are separated from the cortex by a single layer of large parenchyma cells called in the literature either the starch sheath or the endodermis. Within each bundle, an intrafascicular cambium is visible between the xylem and the phloem (see large arrows in Figure 1i). Under our growth conditions, only primary vascular tissues were observed. In contrast, *hca* (Figure 1j) is characterized by a continuous vascular cambium undergoing periclinal divisions leading to radial files of xylem daughter cells that differentiate into secondary xylem (see large arrows in Figure 1j). The presence of primary xylem poles reminiscent of vascular organization typical of wild-type Arabidopsis is still visible immediately inside the ring of secondary xylem (see Xyl in Figure 1h). Surrounding the phloem, we observed the presence of two or three additional layers of parenchyma cells which form a ring inside the starch sheath (see open arrowheads on Figure 1j).

The altered growth pattern in *hca* resulted in a dramatic effect on the surface area of stem tissues. Tissue areas were calculated from digitized images of transverse sections of 20 greenhouse-grown plants at the flowering stage. The total surface area of *hca* stem sections is half that of wild type (0.59 ± 0.08 and 1.37 ± 0.21 mm² respectively). The relative proportions of tissue type were also compared in wild type

and *hca*. The proportion of pith in *hca* is considerably lower (12% in *hca* versus 55% in wild type) with most of the surface area comprising vascular tissue (46% in *hca* versus 20% in wild type).

Abnormal vasculature was observed not only at the base of the stem of *hca* but also at the subapical and middle portions (Figure 1k–n). No interfascicular fibers were present in the subapical zone of *hca*. Parenchyma cells were found in the interfascicular fiber position between enlarged vascular bundles (Figure 1l). In the middle portion of the stem, a continuous ring of xylem/phloem could already be observed (Figure 1n). In contrast, in wild type, as is the case for the basal portion of the stem (Figure 1b,e), triangular vascular bundles alternate with interfascicular fibers forming an arch-shaped pattern around the stem both in the subapical and the middle portion (Figure 1k,m).

The effect of the *hca* mutation on vasculature was further examined throughout the plant. In roots, vascular tissues from *hca* did not exhibit the diarch organization of xylem and phloem typically observed in wild-type plants. Moreover, the diameter of xylem cells was considerably reduced (Figure 2a,b). In 5-week-old hypocotyls, while the majority of the surface area is occupied by secondary xylem in wild-type plants, *hca* exhibited fewer files of xylem with indentations towards the outside of the section. There is no secondary growth apparent, and as a consequence the diameter of the *hca* hypocotyl is smaller than the wild type (Figure 2c,d). This result suggests that the vascular meristems are differentially regulated in shoots and hypocotyls in *hca*.

To investigate if the effect of the *hca* mutation could be observed at younger stages of plant development, we examined the vascular organization of 10-day-old *in vitro*-grown hypocotyls. At the base of wild-type hypocotyls (Figure 2e), the vascular organization is similar to that found in roots; the diarch xylem alternates with the phloem poles. In *hca*, increased cell division was observed within the cambial cells and the pericycle (see large arrows Figure 2f) resulting in an enlargement of the stele throughout the hypocotyl. Taken together, these cytological observations indicate that the *hca* mutation affects cambial activity throughout the plant and leads to altered vascular patterning.

pAthb8::GUS, a marker of procambium specification, is upregulated in hca throughout plant development

To further understand the effects of the *hca* mutation on cambial activity, we monitored the expression pattern of *pAthb8::GUS* (Baima *et al.*, 1995) in an *hca* background. ATHB-8 is a differentiation-promoting transcription factor which regulates the activity of procambial and cambial cells (Baima *et al.*, 2001). Crosses between *hca* and *pAthb8::GUS* plants were performed and the F₂ mutant progeny were analyzed. In the basal portion of 6-week-old

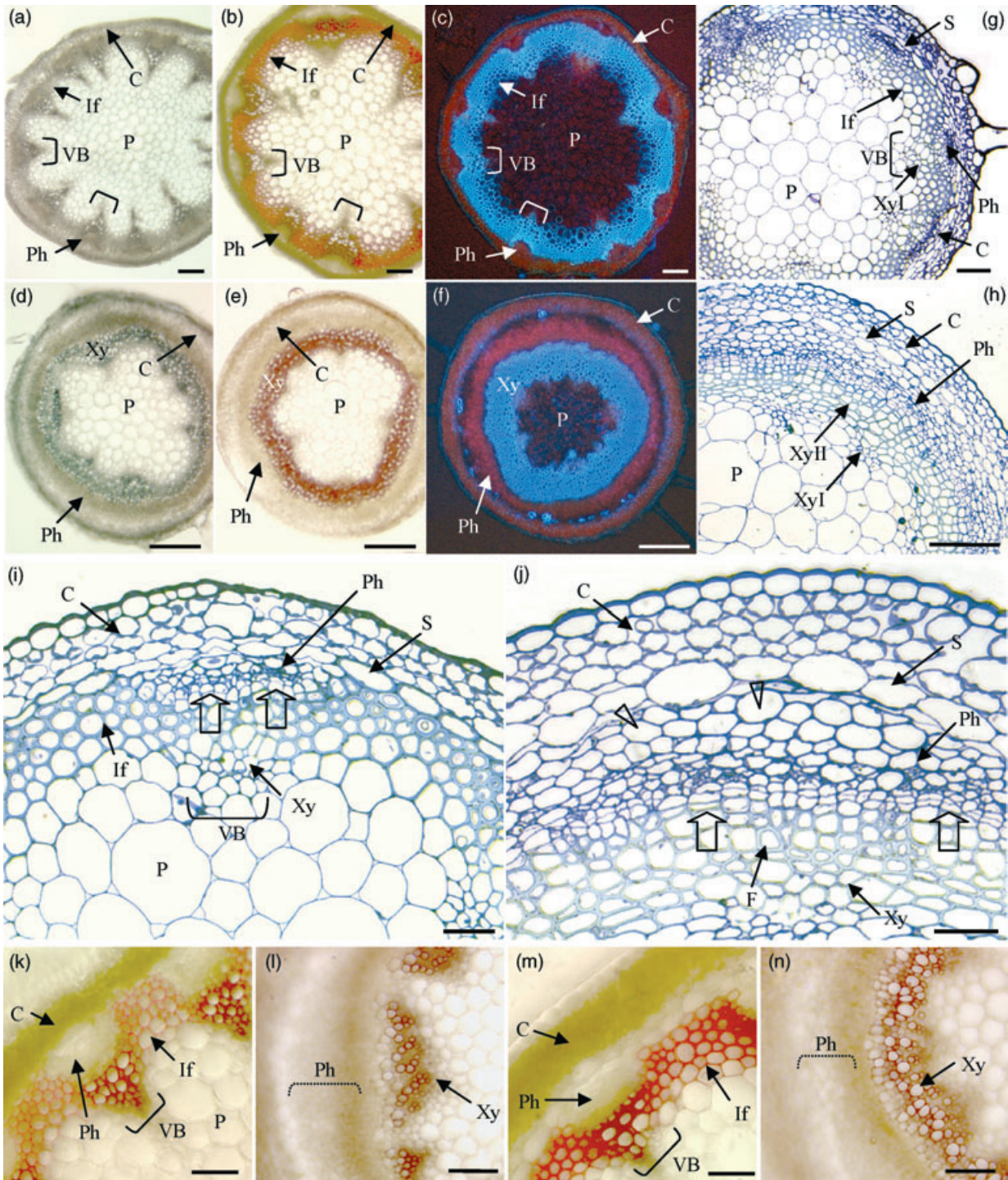


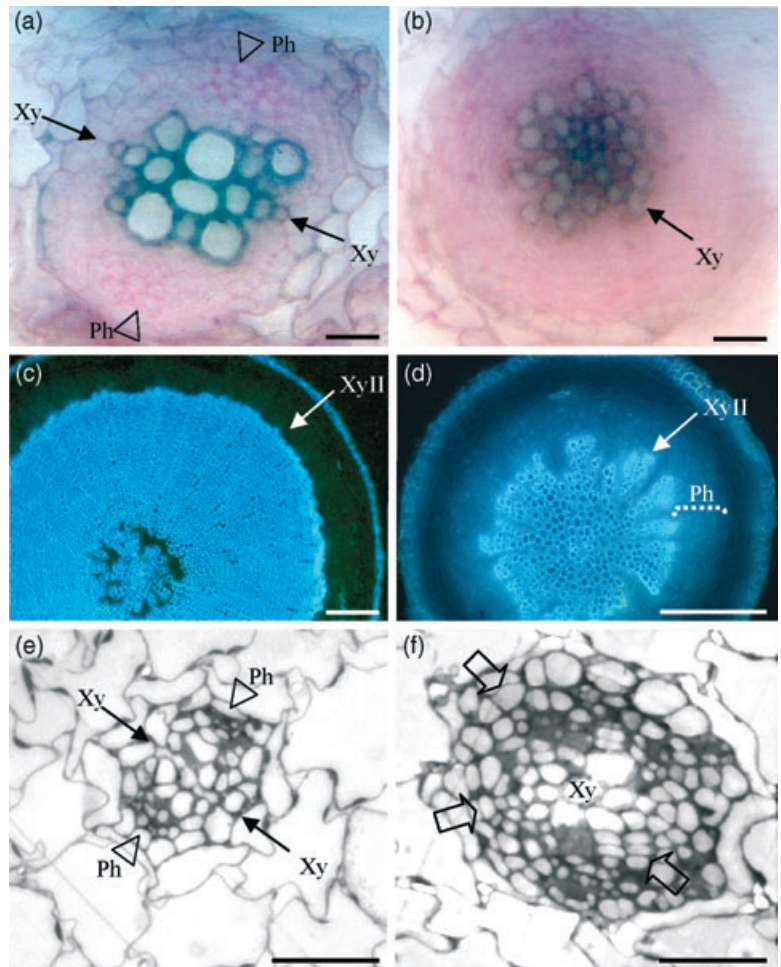
Figure 1. Transverse sections of inflorescence stem of 6-week-old wild type and *hca*: (a–c, g, i, k, m) wild type, (d–f, h, j, l, n) *hca*. (a–f) Hand-cut sections of the basal portion of the stem (a–f) observed under bright field (a, d) or UV light (c, f). Sections were stained with phloroglucinol in (b) and (e). (g–j) Thin sections of the basal portion of the stem stained with toluidine blue. (i, j) Higher magnifications of wild-type and *hca* vascular tissues respectively. A continuous cambium with numerous cell divisions is visualized in *hca* whereas the cambium is restricted to the fascicular region in wild-type stems (see large open arrows in i and j). Open arrowheads in (j) indicate additional parenchyma cells in *hca* between the starch sheath and the phloem. (k–n) Phloroglucinol stained hand-cut sections from the top (k and l) and middle (m and n) portions of the stem. (k) In the top of the wild-type stem, lignified xylem cells in the vascular bundles stained dark red and alternated with lignified interfascicular fibers. (l) In the top portion of *hca* there are no interfascicular fibers and the vascular bundles are wider than the wild type. C, cortex; If, interfascicular fibers; P, pith; Ph, phloem; S, starch sheath; VB, vascular bundle; Xyl, primary xylem; Xyll, secondary xylem, F, fiber cells. Scale bars: (a–h) 100 μ m, (i–n) 50 μ m.

Figure 2. Vascular organization of hypocotyls and roots of wild type and *hca*: (a, c, e) wild type, (b, d, f) *hca*.

(a, b) Transverse section of the stele of 7-day-old roots observed after staining with carmine green. Xylem cells are identified by green staining of their lignified walls whereas phloem cells are stained pink for cellulose.

(c, d) Transverse hand-cut sections of hypocotyls from 5-week-old plants observed under UV light. (e, f) Transverse thin sections in the basal portion of the stele of 10-day-old hypocotyls.

In (a) and (e) the arrows and the arrowheads indicate the xylem and phloem poles respectively. In (f) large arrows indicate extensive division in the pericycle and cambium of *hca*. Ph, phloem; Xy, xylem; Xyll, secondary xylem. Scale bars: (a, b) 30 μ m, (c, d) 100 μ m, (e, f) 50 μ m.



wild-type stems (Figure 3a,b), *ATHB-8* is expressed in parenchyma cells surrounding vessel elements, with only trace amounts of expression in the fascicular cambium (see large arrows in Figure 3b). On the contrary, in the basal portion of *hca* stems (Figure 3c,d), *ATHB-8* is highly expressed in parenchyma cells associated with primary xylem, but also in the continuous cambium (see large arrows in Figure 3d). These results demonstrate an up-regulation of *ATHB-8* in *hca* plants and suggest that the continuous cambium formed as a result of the *hca* mutation is highly active. Interestingly, *ATHB-8* is also expressed in a continuous ring in the subapical portion of the *hca* stem, even prior to the formation of the continuous ring of xylem (Figure 3f). Since *ATHB-8* is expressed during early stages of plant development (Baima *et al.*, 1995), we examined the expression pattern of *pAthb8::GUS* in mature embryos 24 h after imbibition in both *hca* and wild-type backgrounds. A more intense staining is visible in the root apical meristem (RAM) of *hca* as compared with the wild type (Figure 3g,h). The upregulation of *ATHB-8* in the RAM in *hca* suggests that

the *HCA* gene also acts as a regulatory factor in primary meristems. However, it is interesting to note that primary vascular organization in cotyledons and leaves is not altered in *hca* (Figure 3i–l).

The hca mutation has pleiotropic effects on plant morphology

Beyond aspects on vascular patterning, the *hca* mutation caused pleiotropic developmental changes throughout the life cycle. At the flowering stage, *hca* plants are eightfold smaller than wild type and the rosette is composed of twisted, dark-green leaves when grown under long-day conditions (Figure 4a). This difference in rosette morphology is even more pronounced under short-day conditions. *hca* leaves are more twisted and smaller than those of wild-type plants (Figure 4b). Measurements of the morphometric characteristics of 6-week-old plants (Table 1) showed that *hca* plants have very short primary stems (23.8 cm compared with 55.1 cm for wild type). This difference is due to a reduction in internode length. Together with reduced

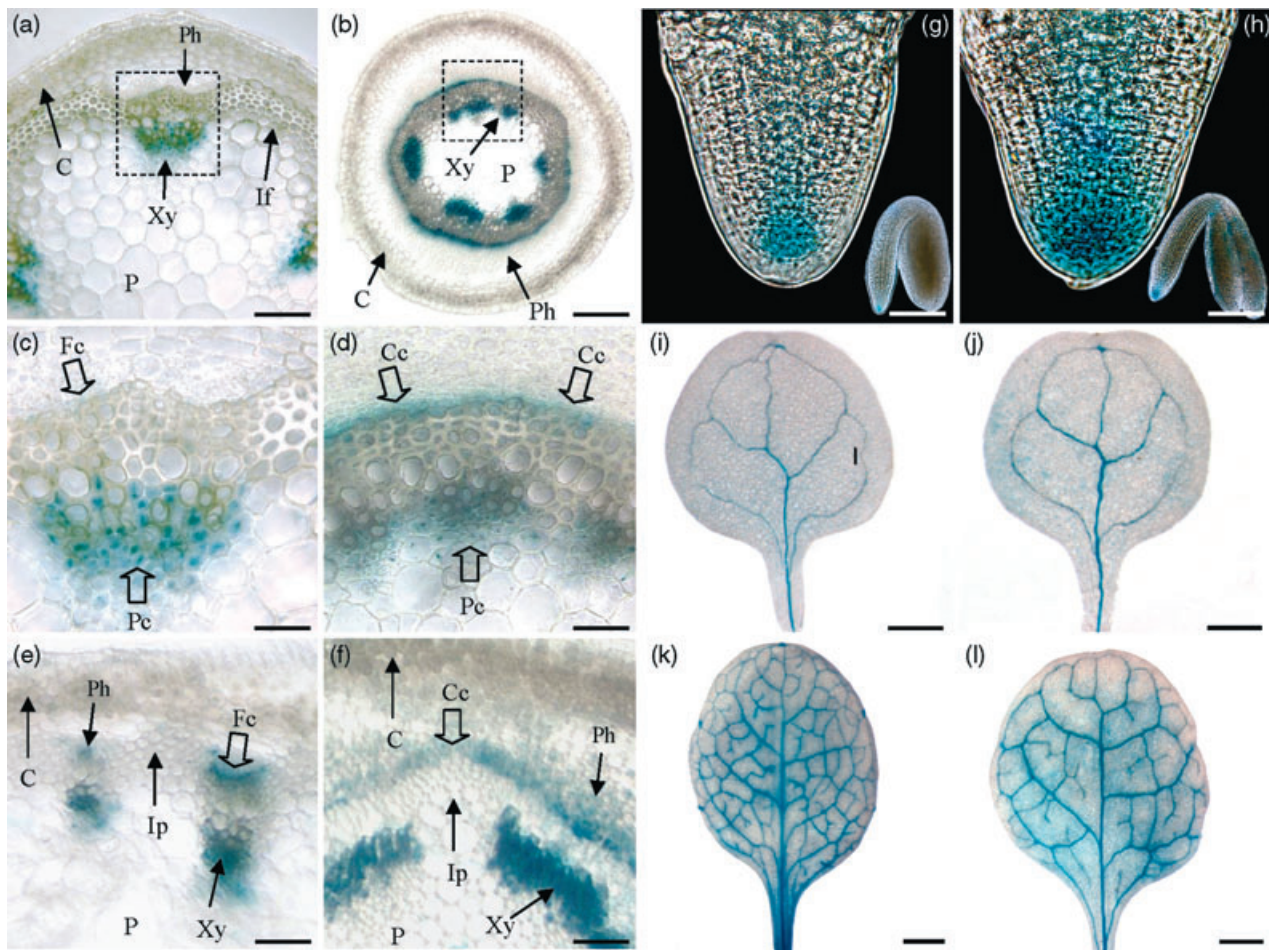


Figure 3. *pAthb-8*:GUS expression in the inflorescence stem, embryo radicle, leaves and cotyledons of wild type and *hca*: (a, c, e, g, j, l) wild type, (b, d, f, h, i, k) *hca*. (a–d) Transverse hand-cut sections from the basal portion of the stem of 6-week-old plants. (e, f) Transverse hand-cut sections from the subapical portion of the stem. In wild-type plants (a, c, e), *pAthb-8*:GUS expression is located in parenchyma cells surrounding primary xylem and to a lesser extent in the fascicular cambium [see large open arrows in (c) and (e)]; (c) corresponds to the boxed-in vascular bundle in (a). In *hca* plants (b, d, f), intense GUS staining is visible throughout the continuous cambium and in parenchyma cells around the primary xylem [see large arrows in (d) and (f)]; (d) corresponds to the boxed-in area of (b). (g, h) Radicle tip of mature embryo imbibed for 24 h. Note the intense GUS staining in *hca* in the root apical meristem (h). (i–l) GUS staining of primary vasculature in leaves and cotyledons of 30-day-old plantlets. C, cortex; Cc, continuous cambium; Fc, fascicular cambium; If, interfascicular fibers; Ip, interfascicular parenchyma; P, pith; Pc, parenchyma cells; Ph, phloem; Xy, xylem. Scale bars: (a, b) 50 μ m, (c, d) 12.5 μ m, (e–h) 5 μ m, (i–l) 1 mm.

internode length, *hca* produced more secondary stems which contribute to the bushy aspect of adult *hca* plants. *hca* flowers were morphologically normal and fertile and the number of siliques per plant was similar in *hca* and wild-type plants (Table 1). *hca* exhibited a continuous but slower growth rate, with a delay in developmental events such as flowering (8 days) and senescence (4 weeks).

The effect of the *hca* mutation was also determined in *in vitro*-grown seedlings. Seven-day-old *hca* seedlings had smaller cotyledons than wild-type seedlings with significantly shorter hypocotyls and roots (Figure 4c,d). A more in-depth examination of hypocotyls using scanning electron microscopy indicated a dramatic reduction in cell size in *hca* plants (Figure 4e,f), suggesting that the mutation

caused a defect in cell elongation. The architecture and development of *hca* roots was also strongly altered: the root of *hca* formed a tripod whereas the wild type produced a long primary root (Figure 4c,d). The tripod is visible between days 4 and 6. The primary root emerges first, followed rapidly by the two other roots; one forms directly at the basal end of the hypocotyl and the second one on the upper portion of the primary root. At day 7, the three roots are of almost equal length. The emergence of lateral roots was delayed by 5 days in *hca* but there was little difference in the number produced (data not shown). When seedlings were grown *in vitro* in the dark, three major differences were observed between *hca* and wild-type plantlets (Figure 4g,h):

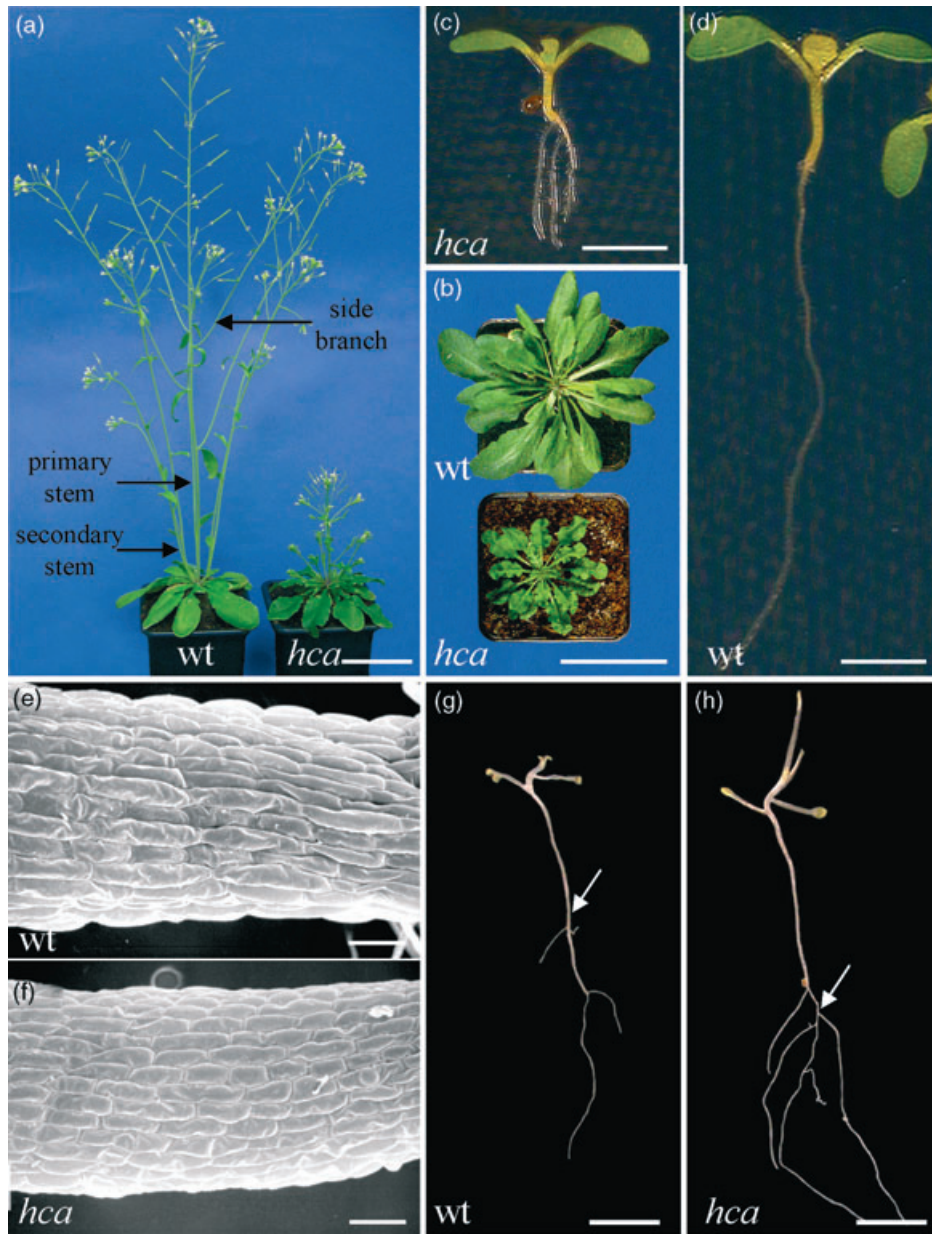


Figure 4. Wild-type and *hca* morphology.

(a) Five-week-old plants grown under long-day conditions. According to the developmental stages of *Arabidopsis* as defined by Boyes *et al.* (2001), after 5 weeks of growth, WT plants were at the 'midflowering stage' whereas *hca* plants were only at the 'first flower open stage'. *Hca* plants are eight times smaller than the wild type.

(b) Five-week-old plants grown under short-day conditions.

(c, d) Seven-day-old *in vitro*, light-grown seedlings.

(e, f) Seven-day-old hypocotyls visualized by scanning electron microscopy.

(g, h) Fourteen-day-old dark-grown *in vitro* seedlings. White arrows indicate roots formed on wild-type hypocotyls and secondary roots in *hca* [(g) and (h) respectively]. Scale bars: (a, b) 5 cm, (c, d) 5 mm, (e, f) 50 μ m, (g, h) 1 cm.

(i) Wild-type seedlings were characterized by an inhibition of secondary root formation whereas secondary root formation in *hca* was stimulated (see white arrow in Figure 4h).

(ii) Short roots appeared on elongated hypocotyls on wild-type seedlings (see white arrows in Figure 4g). In

contrast, the emergence of roots from hypocotyls was never observed on *hca* seedlings.

(iii) Compared with *in vitro* light-grown conditions, the average length of wild-type primary roots is significantly reduced in dark-grown conditions versus light-grown (light 33.6 ± 9.7 mm versus dark 2.6 ± 7.7 mm),

Table 1 Morphometric characteristics of 6-week-old greenhouse-grown wild-type and *hca*

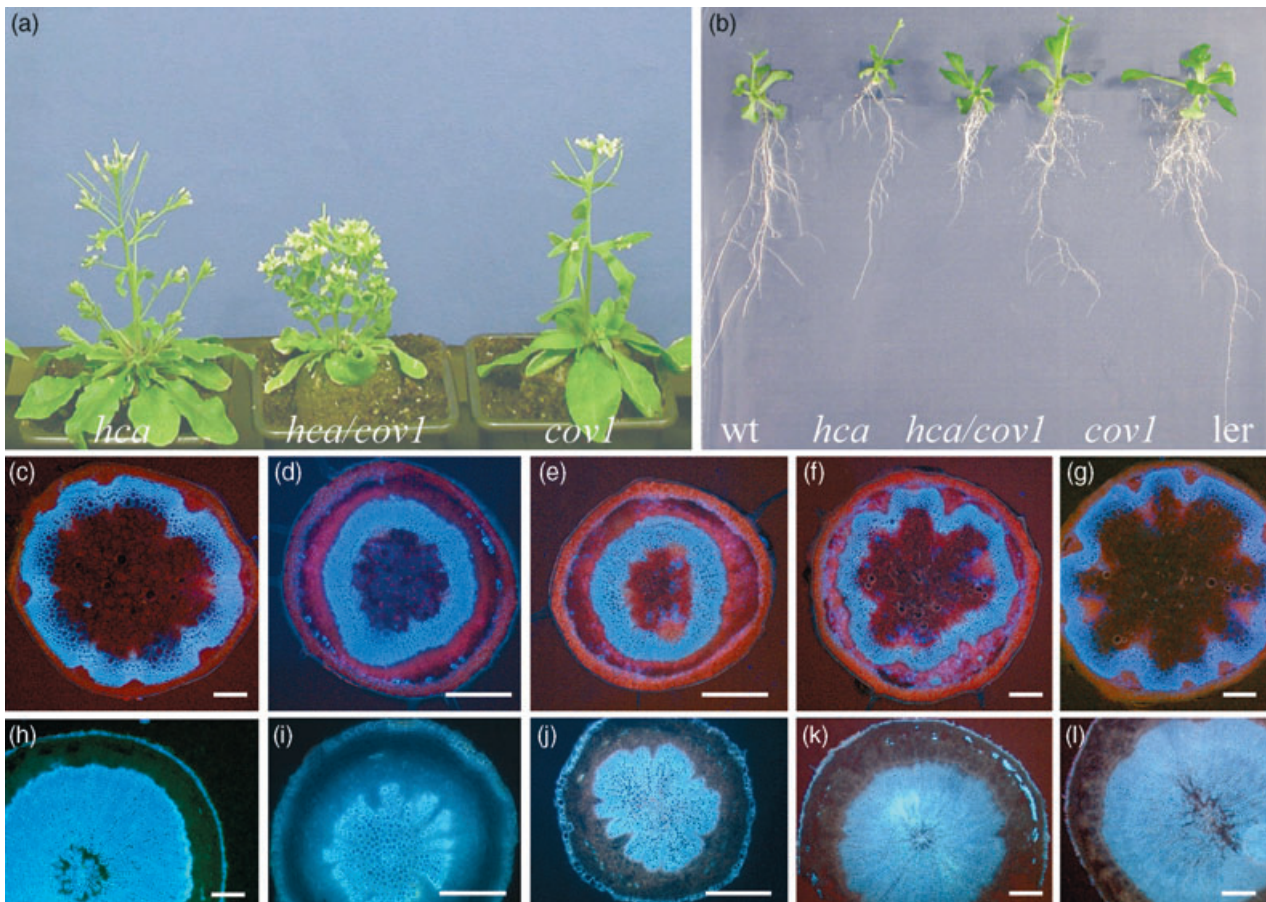
	wt	<i>hca</i>
Primary stem length (cm)	55.1 (2.4)	23.8 (1.8)
Number of side branches	3.3 (0.6)	3.7 (0.4)
Number of secondary stems	4.2 (0.7)	6.0 (2.0)
Number of internodes per stem	3.4 (0.9)	4.1 (0.9)
Internode length (cm)	4.3 (3.4)	1.6 (1.4)
Number of siliques per plant	477.8 (74)	437.1 (56)

Each measurement represents the average of 10 plants. The number in brackets represent the SEM. Number of internodes per stem and internode length were calculated on primary and secondary stems. The sub-apical portion was excluded. Side branches, primary and secondary stems are indicated in Figure 4(a).

whereas the average length of *hca* mains roots is even longer in the dark (light 20.9 ± 7.9 mm versus dark 28.6 ± 8.6 mm).

The vascular organization of the double mutant *hca/cov1* is similar to the *hca* mutant alone

As it has been previously described that the *cov1* Arabidopsis mutant is characterized by a continuous ring of vascular tissue in the stem (Parker *et al.*, 2003), we generated a double mutant, *hca/cov1*. The *hca/cov1* grown in the greenhouse under long-day conditions was shorter and had twisted leaves as compared with *hca* and *cov1* alone (Figure 5a). When grown *in vitro*, roots of 3-week-old *hca/cov1* were twice as short as both single mutants and three to four times shorter than wild-type plants (Figure 5b). Microscopic examination of the stem and hypocotyl vasculature of 6-week-old plants did not reveal any striking differences between *hca/cov1* and *hca* alone, except that the diameter of *hca/cov1* hypocotyls was smaller compared with each mutant individually and both wild types (Figure 5c–l).

**Figure 5.** *hca/cov1* morphology and vasculature organization.

(a) Five week-old plants grown in the greenhouse under long-day conditions.

(b) Three-week-old *in vitro*-grown plants.

(c–l) Transverse stem (c–g) and hypocotyl (h–l) sections of 6-week-old plants. (c, h) WS; (d, i) *hca*; (e, j) *hca/cov1* double mutant; (f, k) *cov1*; (g, l) Ler. Scale bars: (c–l) 100 μ m.

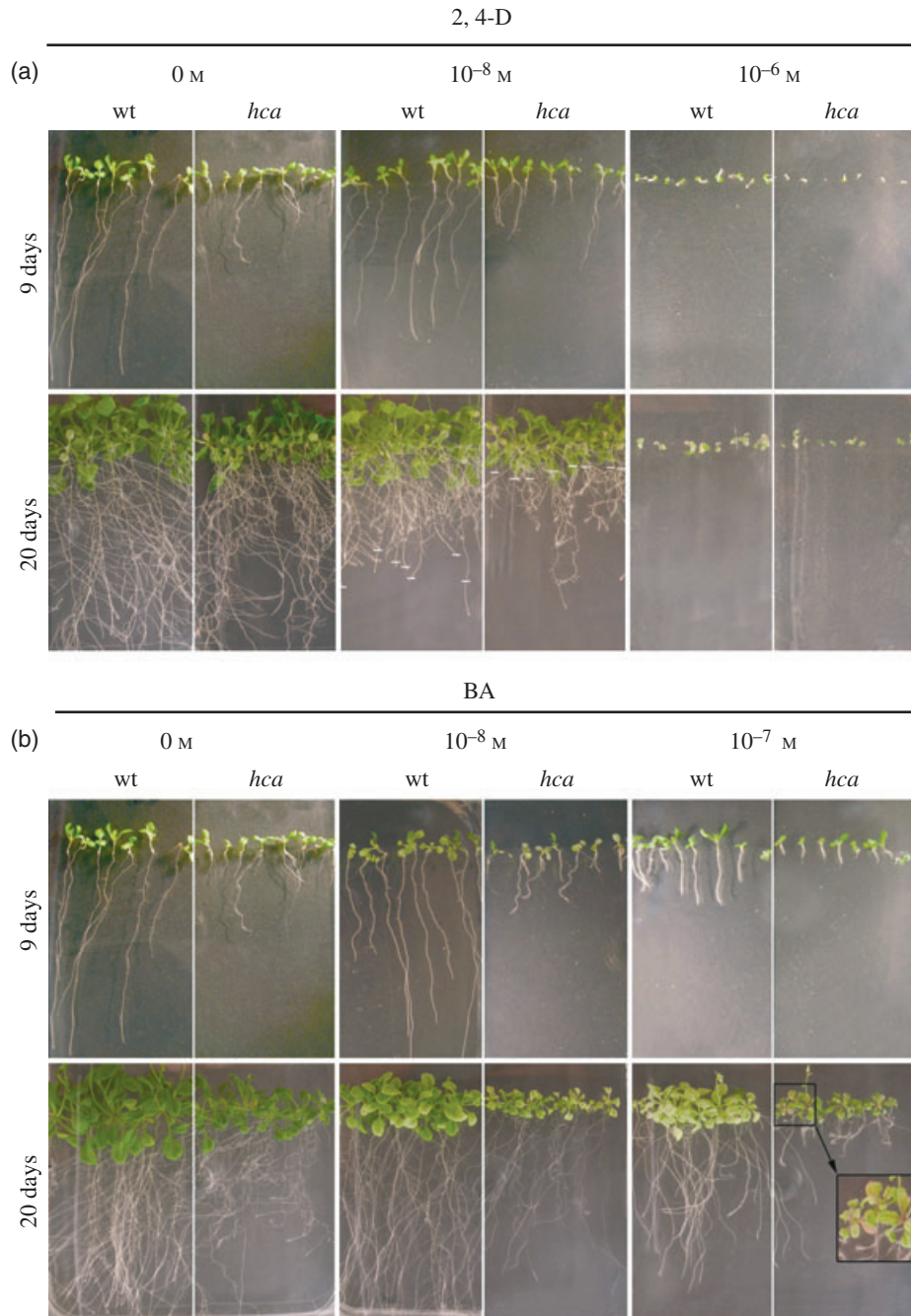


Figure 6. Effect of concentration of auxin and cytokinin in *in vitro* root elongation assays.

Wild-type and *hca* seedlings were grown vertically on plates supplemented with various concentrations of 2,4-D (a) or BA (b). Root growth measurements were performed between day 5 and day 9. The upper rows in both (a) and (b) illustrate seedling growth after 9 days. The lower rows illustrate seedling growth at 20 days. In (a) note the inhibition of root growth in wild-type seedlings in the presence of 10^{-8} M 2,4-D compared with *hca* seedlings between days 9 and 20 (root length at 9 days are indicated by white marks on 20-day-old plants). The average root lengths were as follows: in the absence of hormones, wild type 46.9 ± 7 mm, *hca* 9.4 ± 4.4 mm; in the presence of 10^{-8} M 2,4-D, wild type 29.7 ± 6.8 mm, *hca* 6.9 ± 3.9 mm; in the presence of 10^{-8} M BA, wild type 43.4 ± 7.8 mm, *hca* 5.1 ± 2.5 mm.

The hca mutant displays altered sensitivity towards auxin and cytokinin

The phenotypic modifications caused by the *hca* mutation suggested an alteration in hormonal balance and/or

sensitivity. To assess the role of *hca* in responses to auxin/cytokinin, we first examined root elongation of *in vitro*-grown seedlings in the presence of various concentrations of exogenous auxin (Figure 6a). In 9-day-old seedlings, measurements of root elongation indicated that, in the

presence of 10^{-8} M 2,4-dichlorophenoxyacetic acid (2,4-D), the root elongation of *hca* was proportionally less inhibited (23%) than in wild-type roots (37%) (Figure 6a). This result suggests a lower sensitivity of *hca* to synthetic auxin compared with the wild type. However, at a higher 2,4-D concentration (10^{-6} M), both *hca* and wild-type seedlings were severely affected. Although the seeds germinated, the seedlings did not elongate and became agravitropic (Figure 6a). Interestingly, the difference in sensitivity to auxin between *hca* and wild-type seedlings was accentuated over time. Indeed, when plantlets were grown for 20 days in the presence of 10^{-8} M 2,4-D, *hca* roots continued to grow whereas there was virtually no wild-type root growth between days 9 and 20 (white marks indicate root length at 9 days on Figure 6a). *In vitro* root elongation assays were also performed with two auxin transport inhibitors: TIBA (2,3,5-triiodobenzoic-acid) and NPA (1-naphthalene acetic acid). Root growth of wild-type and *hca* seedlings was inhibited at identical concentrations of TIBA and NPA, and both lines became agravitropic (data not shown), suggesting that basipetal auxin transport was not affected in *hca*. These results were also confirmed by radioactive measurements of polar auxin transport assays (data not shown). In conclusion, the *hca* mutant displays a reduced sensitivity towards exogenous auxin thereby suggesting that the *hca* gene is in some way required for proper auxin perception and/or response. It is noteworthy that all attempts to rescue the *hca* phenotype by the addition of exogenous auxin were unsuccessful.

To elucidate the role of *hca* in cytokinin response, similar root elongation assays were performed in the presence of different concentrations of benzyladenine (BA) (Figure 6b). At day 9, 10^{-8} M BA provoked only very slight effects on the elongation of wild type roots (9% inhibition) whereas at 10^{-7} M, primary root elongation was dramatically inhibited (80%). On the contrary, *hca* root elongation was greatly inhibited even at 10^{-8} M (55% inhibition). The apparent increase in sensitivity of *hca* to BA was also evident when comparing the aerial portions of the plantlets (Figure 6b). Wild-type plantlets grown for 20 days on medium supplemented with 10^{-8} and 10^{-7} M BA were small with pale yellow rosette leaves. At the same BA concentrations, *hca* plantlets were smaller than the wild type and accumulated anthocyanins (Deikman and Hammer, 1995) in the petioles and the basal portion of the stem (see box in Figure 6b). Taken together, these results indicate an increased sensitivity of *hca* to cytokinin, suggesting a role for *HCA* in cytokinin perception and/or response.

The hca mutation affects the response to cytokinin/auxin ratios in in vitro tissue culture assays

In order to more precisely evaluate the role of *hca* in response to auxin/cytokinin, excised hypocotyls from wild-

type and *hca* seedlings were cultured in the presence of various auxin/cytokinin concentrations. When hypocotyl explants were excised from 7-day-old plantlets grown under dim light and cultured for 3 weeks with kinetin and 2,4-D, three main differences could be observed between wild-type and *hca* hypocotyls (see red boxes in Figure 7). Firstly, in the absence of auxin/cytokinin, or at low auxin/cytokinin concentrations (≤ 30 ng ml $^{-1}$) wild-type hypocotyls only produced roots (red boxes with solid line). The first callus from wild-type plants was observed when the medium was supplemented with a minimum of 30 ng ml $^{-1}$ of both hormones. At these hormone concentrations, *hca* hypocotyls never produced roots. Secondly, at elevated 2,4-D concentrations (1000 and 3000 ng ml $^{-1}$) and in the absence of cytokinin, or at low cytokinin concentrations (≤ 30 ng ml $^{-1}$), wild-type hypocotyls elongated and produced small yellow calli at the explant extremities (30 ng ml $^{-1}$ of kinetin). In contrast, hypocotyls of *hca* produced small yellow calli all along the hypocotyls, even in the absence of kinetin (see red boxes with dashed line). Thirdly, at elevated 2,4-D concentrations (1000 or 3000 ng ml $^{-1}$) and kinetin concentrations above 300 ng ml $^{-1}$, callogenesis from wild-type hypocotyls was inhibited at 10 000 ng ml $^{-1}$ of kinetin whereas callus formation from *hca* hypocotyls was inhibited at much lower kinetin concentrations (≥ 300 ng ml $^{-1}$, see red boxes with dotted line). However, the inhibition of callogenesis in *hca* by kinetin was not observed when hypocotyls were grown on media containing auxin concentrations below 1000 ng ml $^{-1}$.

Both the root elongation response and tissue culture experiments indicated that the *hca* mutant displayed a much greater sensitivity to cytokinin, and that this sensitivity is dependent on the concentration of exogenous auxin. Moreover, the capacity of *hca* to induce callus formation in the absence of kinetin suggested that levels of endogenous cytokinin and/or auxin may have been different between *hca* and wild type. Measurements of endogenous IAA and cytokinin content were therefore performed in both the aerial parts and roots of 15-day-old wild-type and *hca* plants (Figure 8).

As for cytokinins (Figure 8a), a reduced level of isopentenyladenosine-5'-monophosphate (iPMP) was observed in *hca* shoots as compared with wild type. The pool sizes of zeatin-type cytokinin were unchanged in the shoot of the mutant. In roots, (Figure 8b) zeatin ribotide (ZMP), zeatin riboside (ZR) and zeatin-O-glucoside (ZOG) were all significantly less abundant in *hca*. The levels of iP-type cytokinins were not altered in *hca* roots. For IAA, the content was slightly lower in both roots and shoots in the *hca* mutant in comparison with wild type (Figure 8c). A lower level of IAA in the *hca* mutant was also observed in hypocotyls of adult plants (*hca* 108 ± 13 ng g $^{-1}$ fresh weight; wild type 198 ± 59 ng g $^{-1}$ fresh weight). In contrast, there was no difference in IAA content in the upper part of the inflorescence

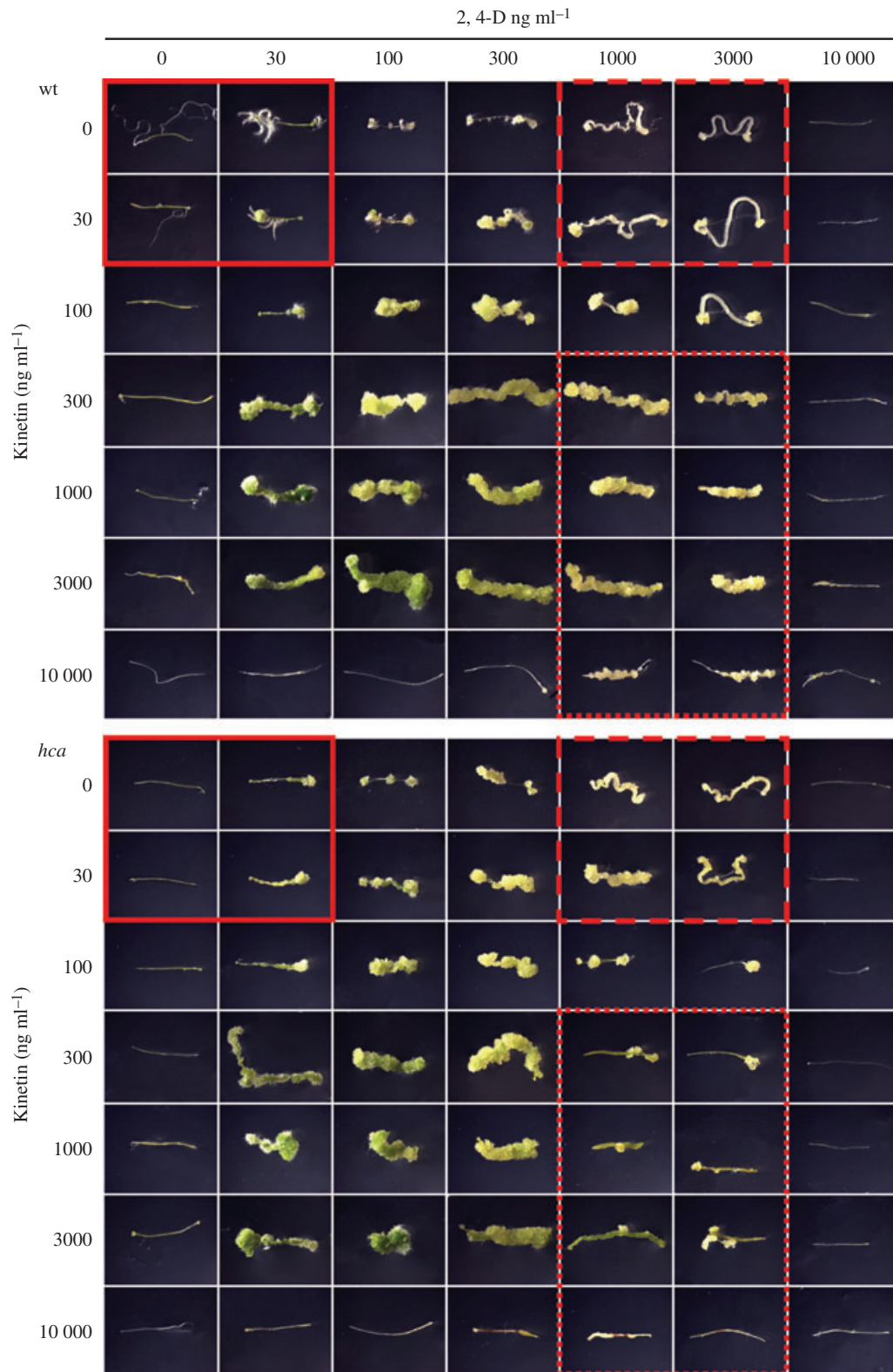


Figure 7. The Effect of auxin and cytokinin concentration on excised hypocotyls of wild-type and *hca* seedlings. Hypocotyls were excised from seedlings grown under reduced light for 7 days and transferred to media containing various concentrations of 2,4-D and kinetin for 3 weeks. Ten hypocotyls of each genotype were examined for each hormone combination.

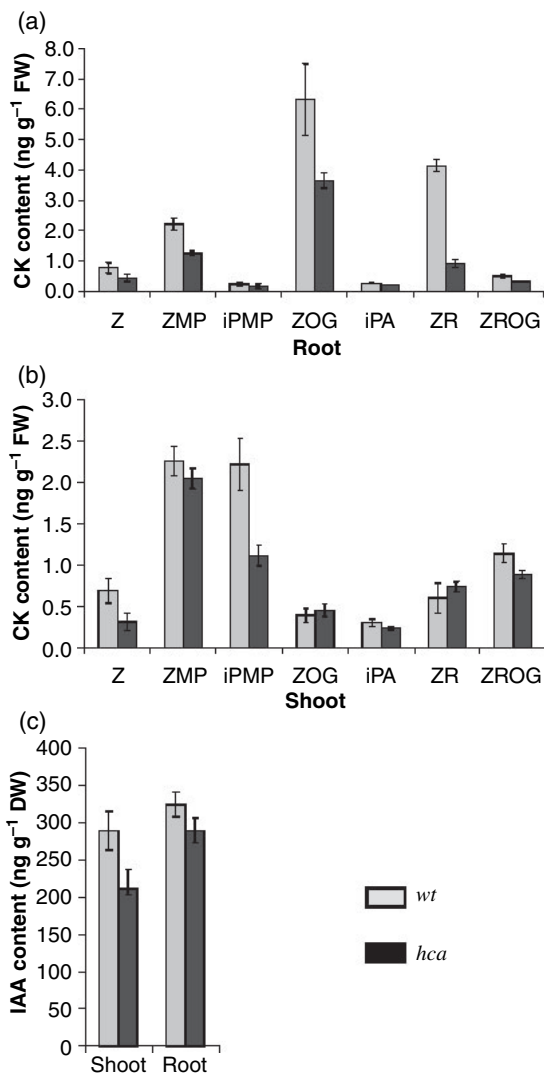


Figure 8. Auxin and cytokinin content in 15-day-old wild-type and *hca* seedlings grown *in vitro*.

(a, b) cytokinin content in shoots and roots respectively.

(c) IAA content in shoots and roots. Error bars represent standard deviations. Abbreviations: Z, zeatin; ZMP, zeatin riboside-5'-monophosphate; iPMP, isopentenyladenosine-5'-monophosphate; ZOG, zeatin-O-glucoside; iPA, isopentenyl adenosine; ZR, zeatin riboside; ZROG, zeatin riboside-O-glucoside.

and just below the lowermost leaf (data not shown). In conclusion, the *hca* mutation leads to a reduced levels of the major zeatin-type cytokinins and IAA levels in young *hca* plantlets compared with wild type.

Microarray analysis sheds light on certain aspects of the *hca* phenotype

To determine the influence of the *hca* mutation on global gene expression, transcriptome profiling was performed on 10-day-old WS versus *hca* mutant plantlets using the

complete Arabidopsis transcriptome microarray (CATMA) (Crowe *et al.*, 2003). The CATMA contained 24,576 GSTs corresponding to known and predicted genes. In 10-day-old *hca* plantlets, a total of 239 genes (about 1% of the genes on the array) had a significant differential expression, with 165 genes upregulated and 74 downregulated. These genes are listed in Supplementary data S1. Interestingly, among the 165 upregulated genes, a large proportion of cell wall-related genes were identified (expansins, extensins, chitinases, arabinogalactan proteins, hydroxyproline-rich proteins etc.). Another striking feature of *hca* gene expression is the upregulation of several members of the zinc finger transcription factor family, mainly the C3HC4 type and the Dof type. Some Dof transcription factors have been shown to be specifically expressed in the vascular system of plants (Papi *et al.*, 2002). Interestingly, the most upregulated transcription factor belongs to the Scarecrow transcription factor family (At4g36710) which plays an essential role in the radial patterning of both roots and shoots (Wysocka-Diller *et al.*, 2000). A second Scarecrow-like protein is also upregulated, but to lesser extent. An AP2 domain-containing transcription factor (At3g57600) which interacts with scarecrow, is also upregulated in *hca* (Aida *et al.*, 2004).

In support of the physiological data indicating that *hca* has an overall altered response to auxin/cytokinin and an enhanced sensitivity to cytokinin, we found that Arabidopsis response regulator 16 (ARR16; At2g40670) was upregulated in *hca*. ARR16 belongs to the type A ARR gene family (Kiba *et al.*, 2002) and is involved in the AH4 histidine kinase-mediated cytokinin signaling pathway in Arabidopsis roots. It is also one of the most strongly and rapidly upregulated genes in response to exogenous cytokinin treatment on seedlings (Rashotte *et al.*, 2003). To a lesser extent an 'auxin-response protein-related' gene is also upregulated in *hca*.

Genetic analysis and *hca* mapping

hca was originally isolated as a T-DNA-tagged mutant from the INRA Versailles collection (Beschold *et al.*, 1993). The homozygous mutant line was backcrossed with wild-type WS and the resulting F₁ progeny was selfed. PCR and kanamycin segregation tests on the F₂ progeny revealed that the T-DNA and the *hca* phenotype were not linked. Segregation of different phenotypic traits of *hca* including twisted leaves and abnormal vasculature was performed by analysing 174 F₂ progeny. A 100% correlation was observed between twisted leaves and abnormal vasculature and the repartition of these characters was very near to 25% of the total plant population (22.4%) (χ^2 , $\alpha < 5\%$). These results indicated that the overall *hca* phenotype is due to a monogenic, recessive mutation. The localization of the *hca* locus was undertaken by generating an F₂-mapping population by crossing the *hca* line with Columbia Arabidopsis Col-0. Ninety-eight mutants were isolated and screened with SSLP

(simple sequence length polymorphism) markers spanning the entire Arabidopsis genome (Bell and Ecker, 1994; Ponce *et al.*, 1999). The *hca* mutation was located on the lower arm of chromosome 4 between nga1107 (10.5 cM) and nga1139 (4.9 cM). For more detailed mapping, additional SSLP markers were generated within the region containing the *hca* mutation. These SSLP markers were used to screen a test cross population to identify critical recombination near the mutation. The test cross population was generated by two successive crosses. The first cross was made between *hca* and Col-0 wild-type plants and the second between the F₁ progeny of the first cross and *hca*. The phenotype of plants from this population was 50% mutant and 50% wild type (heterozygous). More than 1500 plants were screened with these additional SSLP markers. This allowed us to reduce the mutated region to 240 kb. This region contains 68 predicted open reading frames (ORFs) from *At4g35295* to *At4g35940*. As no supplementary recombination was observed in this region, another recombinant population is currently being constructed using a line containing a T-DNA in one of these ORFs. The presence of the T-DNA will enable us to use kanamycin resistance as a phenotypical marker to screen the population.

Discussion

hca is characterized by abnormal cambial activity leading to an altered pattern of vascular tissues. In inflorescence stems, an interfascicular cambium is formed very early in development, resulting in the production of large amounts of vascular tissue (46% in *hca* versus 20% in wild type). As a consequence, *hca* does not exhibit the alternate vascular bundle/sclerenchyma fiber organization typically observed in wild-type plants. Instead, a continuous ring of vascular tissue with some sclerenchyma fibers dispersed throughout the ring was observed. This vascular organization is reminiscent of the vasculature of herbaceous species with secondary growth, i.e. tobacco and woody species. However, in contrast to woody species, this extensive secondary growth is not accompanied by an enlargement of the stem diameter. Interestingly, despite the fact that *hca* acts early during plant development as observed by upregulation of *ATHB-8* in root meristem and increased cell division in 10-day-old hypocotyls, the organization of primary xylem in stems, *sensu stricto*, was not modified. Indeed, the xylem poles were correctly positioned under the ring of secondary xylem. We therefore hypothesize that *hca* exhibits premature secondary growth. A continuous ring of vascular tissue has been described in the stem of the Arabidopsis mutant, *cov1* (Parker *et al.*, 2003). The *COV1* gene encodes a membrane protein of unknown function. In keeping with the *cov1* phenotype, the fact that auxin response was not altered, and that auxin content was two times lower in the hypocotyl, the authors suggested that the *COV1* gene could be involved in a

mechanism that negatively regulates the differentiation of vascular tissues. Based on the map position, *HCA* is not allelic to *COV1*. Moreover *hca* exhibited significant differences in the organization of the vasculature compared with *cov*. In stems *hca* vasculature forms a continuous ring of secondary tissues, whereas the *cov* vasculature still exhibits arch-shaped vascular bundles and no secondary growth. In mature hypocotyls there is no difference in secondary xylem formation between *cov* and wild type, whereas *hca* produced less xylem compared with wild type. The vasculature of the double mutant *hca/cov* is more similar to *hca* than to *cov* in both stems and hypocotyls. However, the alteration of vasculature of *hca/cov* was no greater than either mutant alone. Based on this observation we cannot conclude to whether *HCA* and *COV* act in the same pathway or not.

Previous studies on aspen have clearly underlined the role of auxin on cambial activity and subsequent secondary growth (Sundberg *et al.*, 2001; Uggla *et al.*, 1996). Furthermore, several Arabidopsis mutants impaired in auxin response or transport that exhibit alterations in vascular differentiation or patterning have been described (for reviews see Berleth and Mattsson, 2000; Berleth *et al.*, 2000; Hobbie, 1998). In this context, we performed an in-depth examination of the auxin status in the *hca* mutant. Different experimental assays pointed to an altered response to auxin in *hca*. Firstly, in root elongation assays, *hca* is less sensitive to exogenous auxin than the wild type. Secondly, in tissue culture experiments, although callus formation could be induced at the same auxin concentration in wild-type and *hca* hypocotyls, the inhibition of callogenesis in *hca* was observed at lower auxin concentrations than in the wild type. These results indicate that the response to auxin in *hca* is altered in an organ-specific manner. This alteration in auxin response is not directly related to auxin transport, since auxin transport is not affected in *hca*. Moreover, both the vascular alteration and overall phenotype of *hca* are different from that in mutants affected in auxin transport, such as *pin* (Gälweiler *et al.*, 1998) and *lop* (Carland and McHale, 1996), auxin-inducible genes, such as *iaa/axr* (Hobbie *et al.*, 2000), or transcription factors that regulate these genes, such as *monopteros* (Berleth and Jürgens, 1993). At present, a direct link between altered vascular patterning and auxin response and content in *hca* cannot be established.

Many of the phenotypic characteristics of *hca*, including delay of leaf senescence, loss of apical dominance and inhibition of hypocotyl elongation, suggest an altered cytokinin metabolism and/or response to cytokinin (for review see Mok and Mok, 2001). We have therefore performed a detailed investigation of the effect of exogenous cytokinin in various *in vitro* assays. Normally, the addition of exogenous cytokinin to plants grown *in vitro* induces callogenesis and inhibition of root primordia and root hair formation. Interestingly, all of these cytokinin responses were observed in

hca in the absence of cytokinin. Moreover, callus formation was severely inhibited at a cytokinin concentration 30 times lower in *hca* than in the wild type. The increased sensitivity of *hca* to exogenous cytokinin was also observed in *in vitro* plantlets. An inhibition of root growth and a pronounced accumulation of anthocyanin in leaves were observed at a lower BA concentration compared with wild type.

Taken together, these results suggested that *hca* was either an overproducer of cytokinin or had an increased sensitivity to cytokinin. Interestingly, our analysis of cytokinin pool sizes revealed a clear downregulation of the pathway involving zeatin-type cytokinins while the iP-related pathway was more or less unaltered. This effect on cytokinin homeostasis suggests that the suppression of cytokinin biosynthesis in *hca* could be explained by potential crosstalk between homeostasis and signal transduction; basically, a hypersensitivity to cytokinin could induce feedback inhibition of the synthesis. The fact that the cytokinin content in *hca* plantlets was even lower than in the wild type thereby favors the increased response hypothesis. We postulate that *hca* could interfere directly or indirectly with mechanisms regulating cytokinin response and may act as a switch in maintaining the downstream cytokinin signaling cascade in the 'on' position (i.e. in a constitutive fashion). In support of this hypothesis, microarray analysis of *hca* indicated that the gene *ARR16* involved in cytokinin response (D'Agostino *et al.*, 2000; Kiba *et al.*, 2002; To *et al.*, 2004) was upregulated in *hca* plantlets. This gene was also shown to be upregulated in wild-type plantlets treated with exogenous BA (Rashotte *et al.*, 2003). In this way, constitutive activation of the cytokinin pathway could conceivably lead to a hypersensitivity to exogenous cytokinin. This hypersensitivity might induce a feedback regulation that in turn decreases the cytokinin levels observed in the *hca* mutant.

An increase in cytokinin sensitivity has already been described in two types of mutants affected in their cytokinin signaling pathways. Kubo and Kakimoto (2000) reported that calli produced by *ckh1* and *ckh2* exhibited typical cytokinin responses at lower levels of kinetin than in wild type. The authors speculate that *CKH1* and *CKH2* gene products negatively regulate the signaling pathway of cytokinin perception that leads to cell proliferation and chloroplast development. That said, beyond the cytokinin response, *ckh* mutants do not exhibit an altered vascular system (C. Pineau, unpublished data). Recently, the family of ARR genes has also been characterized as negative regulators of the cytokinin signaling pathway since the inhibition of root elongation in response to cytokinin is more sensitive in a multiple *arr* mutant than in wild type (To *et al.*, 2004). However, with the exception of delayed leaf senescence, both the multiple *arr* mutants and the *ckh* mutant are phenotypically very different from *hca*. To date, we cannot conclude if an altered cytokinin response is a primary or secondary effect of the *hca* mutation. Keeping in mind that

auxin promotes and is required for cell division in the cambium, it is also tempting to speculate that the activation of cambial cell division in the interfascicular region of *hca* stems is a result of an enhanced sensitivity of these cells to cytokinin. Cytokinin is well known for its role in the cell cycle (D'Agostino and Kieber, 1999) and Shibaoka (1994) reported that cytokinin influences the plane of cell division with an increased number of periclinal rather than anticlinal divisions.

Taken together, the physiological data presented here suggest that the *hca* mutation leads directly or indirectly to an enhanced sensitivity toward cytokinin, and as a result a modification of the response to auxin and cytokinin. In this way, we hypothesize that auxin response of *hca* could be a secondary effect of the mutation and should be viewed in an integrative response scheme that may include other hormones and environmental factors. For example, interaction between light and cytokinin signaling pathway has been described in the *det1* mutant (Chory *et al.*, 1994), and more recently Cluis *et al.* (2004) reported that the transcription factor HY5 integrates light and auxin signaling pathways. In keeping with these observations, it is interesting to note that light had a significant effect on the root phenotype of *hca*. When grown under light conditions, the emergence of secondary roots is delayed in *hca* when compared with wild type. In contrast, under dark-grown conditions, *hca* seedlings exhibit enhanced root formation. Synergistic, antagonistic and additive interactions among plant hormones have been demonstrated in many aspects of plant development (Coenen and Lomax, 1997; Nordström *et al.*, 2004). Mutants that respond abnormally to one phytohormone often respond abnormally to others, reflecting the complex interacting network of hormone response pathways. Alterations in auxin and cytokinin responses associated with abnormal vascular organization have been described in the rice mutant *ral1* (Scarpella *et al.*, 2003) and the *pls* mutant in Arabidopsis (Casson *et al.*, 2002). The *ral1* mutant is impaired in procambial development and exhibits altered leaf venation patterning. To date the *RADICLELESS1 (RAL1)* gene has not yet been cloned, but physiological data indicated that the gene may play an important role in the establishment of vascular patterns and proper response to auxin and cytokinin. In the same way, the *POLARIS (PLS)* gene which encodes a small peptide (Casson *et al.*, 2002) is required for correct auxin-cytokinin homeostasis to modulate leaf vascular patterning. Based on the map position of *HCA*, it is unlikely that *HCA* is allelic to *POLARIS*.

To date, the molecular nature of the *HCA* gene product is not known. Thus, it is possible that the *hca* mutation directly affects a step in the cytokinin transduction pathway. Alternatively, as *hca* exhibited a pleiotropic phenotype it is also possible that the *hca* gene is involved in a very early step in controlling plant development by acting on the commitment of cambial cells via

modification of hormone sensitivity. As a consequence, extensive cell division could occur in both the fascicular and interfascicular regions leading to early and increased secondary growth in stems. One attractive model would be that *hca* gene interacts with *INTERFASCICULAR FIBERLESS1* (Ratcliffe *et al.*, 2000; Zhong and Ye, 1999; Zhong *et al.*, 1997) to control the status of cell division and differentiation in the interfascicular region in the stem. The fact that *hca* is characterized by few fibers and that these are dispersed throughout the xylem ring supports this hypothesis. The future cloning of the *hca* gene will allow us to establish the link between proper response to auxin and cytokinin and vasculature development.

Experimental procedures

Plant material and mutant isolation

Microscopic screening was performed on 4-week-old plants from T-DNA-mutagenized T₂ lines of *Arabidopsis thaliana* (Beschta *et al.*, 1993). Hand sections of 12 different plant stems per line were observed under bright field and UV light, or stained with phloroglucinol according to standard protocols (Nakano and Meshitsuka, 1992).

The *pAthb-8::GUS* seeds were provided by the Arabidopsis Biological Resource Center (Ohio State University, Columbus, OH, USA).

The double mutant, *hca/cov1*, was obtained by crossing homozygous *hca* and *cov1* lines. The first generation (double heterozygotes) was selfed and the double homozygous mutant *hca/cov1* was identified using SSLP genetic markers designed for mapping the two mutants. This screening method was possible since *hca* is in a WS genetic background and *cov1* in a Ler (Landsberg erecta) background.

Growth conditions for seedlings and adult plants

Seeds were surface-sterilized for 25 min in sterile water containing 25% bleach and 0.1% Triton X-100, and washed three times in sterile water. The seeds were then imbibed in 0.2% agarose for 2 days at 4°C in the dark and subsequently sown on the basal growth medium composed of 4.32 g l⁻¹ Murashige and Skoog medium (Sigma Lyon, France, M5519), 1% sucrose, 10 ml l⁻¹ of 5% 2-(*N*-morpholino) ethane sulfonic acid pH 7.5, 100 mg l⁻¹ inositol, 10 mg l⁻¹ thiamine-HCl, 1 mg l⁻¹ pyridoxine-HCl, 1 mg l⁻¹ nicotinic acid and 0.6% phytigel (Sigma). For phenotypic observations and root elongation assays, seedlings were grown vertically on Petri plates either under light conditions (16 h at 100 μmol m⁻² sec⁻¹) or in the dark at 20°C. For *in vitro* callogenesis assays, hypocotyls were excised from plants grown for 7 days in dim light.

When plants were grown to maturity, seeds were sown directly in Giffy mottes and grown in the greenhouse. Plants were irrigated once a week with nutrient solution.

Microscopy

Stems and hypocotyls were fixed in 2.5% glutaraldehyde, 3% paraformaldehyde and 0.1 M sodium phosphate (pH 7.3). After

fixation, plant material was rinsed in 0.1 M sodium phosphate (pH 7.3) and a secondary fixation procedure was performed with 1% osmium tetroxide prepared in 0.1 M sodium phosphate (pH 7.3) solution. Tissues were rinsed and dehydrated in a successive ethanol series (10, 30, 50, 70, 95, 100%), and infiltrated step-wise with Spurr resin (25, 50, 70, 100% in ethanol). Sections 1 μm thick were stained with 1% toluidine blue (w/v).

Hand-cut sections from fresh *Arabidopsis* stems or roots were observed using an inverted Leica microscope (Leitz, Rueil-Malmaison, France, DMIRBE), equipped with epifluorescence illumination (excitation filter BP 340–380 nm, suppression filter LP 430 nm). Images were registered using a CDD camera (Colour Coolview, Photonic Science, Robertsbridge, UK) and treated by image analysis (Image Pro-plus, Media Cybernetics, Silver Spring, MD, USA).

In vitro root elongation assays

Root elongation assays were performed on seedlings germinated on MS medium described above in the presence of various concentrations of 2,4-D or BA. Root length was marked on Petri plates and growth was measured between 5 and 9 days. Plates were photographed at 9 and 20 days. For *hca*, root length was considered as the mean length of the three roots comprising the tripod root. Hormonal stimulation or inhibition of root elongation for wild type and *hca* was calculated as a percentage of root elongation on hormone-free MS medium. These per cent values were used to compare the hormone response of wild type and *hca*. Lateral root emergence was quantified at 12 days.

In vitro callogenesis assays

Hypocotyls from 7-day-old wild-type and *hca* seedlings were excised and placed on basal medium as described above, supplemented with 1 mg l⁻¹ of biotin and various concentrations of the kinetin and 2,4-D. Hypocotyls were cultivated for 3–4 weeks at 23°C under light conditions (16 h day length at 100 μmol m⁻² sec⁻¹). Ten hypocotyls were tested for each combination of hormone concentrations. A representative callus for each hormonal concentration was photographed.

Measurements of endogenous cytokinin and IAA content

Endogenous IAA measurements on 15-day-old *in vitro*-grown plantlets were performed using the isotope dilution MS method according to Edlund *et al.* (1995). Frozen plant material was ground with a mortar and pestle in liquid nitrogen. For cytokinin analysis, tissue was extracted in the extraction buffer MeOH:H₂O:HCOOH (15:4:1 v/v) for 2 h (–20°C) in the presence of heavy labeled internal standards ²H₅-Z, ²H₅-ZR, ²H₅-Z9G, ²H₅-Z7G, ²H₅-ZOG, ²H₅-ZROG, ¹⁵N-²H₅-ZMP, ²H₆-iP, ²H₆-iPA, ¹⁵N-²H₆-iPMP (Z, zeatin; ZMP, ZR-5'-monophosphate; iPMP, isopentenyladenosine-5'-monophosphate; ZOG, zeatin-*O*-glucoside; iPA, isopentenyl adenosine; ZR, zeatin riboside; ZROG, zeatin riboside-*O*-glucoside). Cytokinins were purified as described by Nordström *et al.* (2004) and derivatized as described in Åstot *et al.* (1998). Cytokinin analysis by mass spectrometry was performed in selective reaction monitoring mode. Chromatographic separation was performed using a drop-in guard cartridge 10 × 1 mm BetaMax Neutral, with 5 μm particle size (Thermo Hypersil-Keystone, Cambridge, UK) as analytical column. Before loading samples in the autosampler the propionylated samples were dissolved in 1.3 μl acetonitrile containing 3% formic acid followed by 11.7 μl H₂O also containing 3% formic acid. At a

flow rate of 10 $\mu\text{l min}^{-1}$ the following binary gradient was used: 0 to 2 min, isocratic elution of 5% solvent B; 2 to 10, a linear gradient to 55% B; followed by isocratic elution of 55% solvent B. After analysis, the column was washed by 100% solvent B at a flow rate of 80 $\mu\text{l min}^{-1}$ and equilibrated for initial conditions. Solvent A consisted of 3% (v/v) formic acid in water, and solvent B consisted of 3% (v/v) formic acid in acetonitrile. Effluents from the chromatographic column were introduced to a Micromass Quattro Ultima mass spectrometer (Micromass, Manchester, UK) via an electrospray ion source. The following mass spectrometric set-up was used: capillary voltage +3 kV, source temperature 90°C, desolvation temperature 250°C, cone gas flow 12 l h⁻¹, desolvation gas flow 800 l h⁻¹. The collision cell pressure was kept between 2 and 2.5 mbar with argon gas and the cone voltage and collision cell energies were as follows [cone voltage (V)/collision cell energy (eV)]: Z (60/14), iP (60/15), PRO-Z (60/14), PRO-DHZ (60/17), PRO-ZR (60/19), PRO-iPA (80/17), PRO-ZOG (80/25), PRO-iPMP (80/18), PRO-ZMP (80/20), PRO-DHZR (60/19), PRO-Z7G,Z9G (100/22), PRO-ZROG (85/27). Data were processed using Masslynx software (Micromass, Manchester, UK).

Localization of GUS activity

GUS activity analysis was performed according to Jefferson *et al.* (1987) in a homozygous *hca* line containing a *pAtha-8::GUS* construct. Briefly, sections were hand-cut or mature embryos were pulled out from their tegument after 1 night's imbibition and incubated for several hours to overnight in 2 mM X-Gluc (5-bromo-4-chloro-3-indolyl- β -D-glucuronidase), 0.1% Triton X-100, 50 mM sodium phosphate pH 7.0, and 1 mM each of K⁺ ferri/ferrocyanide. Depending of tissue toughness (old leaves, floral stems), an additional vacuum infiltration step was performed with the same reaction medium for 10 min before incubation. After the reaction, the GUS staining was fixed for 1 h in 5% formaldehyde, 5% acetic acid and 45% ethanol. Green tissues were depigmented in 70% ethanol.

Microarray analysis

The microarray analysis was performed with the CATMA array containing 24576 gene-specific tags (GSTs) from *A. thaliana* (Crowe *et al.*, 2003; Hilson *et al.*, 2004). The GST amplicons were purified on Multiscreen plates (Millipore, Bedford, MA, USA) and resuspended in Tris EDTA-DMSO at 100 ng μl^{-1} . The purified probes were transferred to 1536-well plates with a Genesis workstation (TECAN, Männedorf, Switzerland) and spotted on UltraGAPS slides (Corning, New York, NY, USA) using a Microgrid II (Genomic Solution, Huntingdon, UK). The current CATMA version printed at the Unité de Recherche en Génomique Végétale (URGV) consists of three metablocks, each composed of 64 blocks of 144 spots. A block is a set of spots printed with the same print-tip. In these arrays, a print-tip is used three times to print a block in each metablock.

For the transcriptome studies, whole seedlings were harvested at 10 days after germination, at the stage where cotyledons opened fully according to Boyes *et al.* (2001) from 3 \times 300 plants of *A. thaliana* WS and *hca*. One dye swap was performed for each biological replicate. Plants were grown *in vitro* on Petri plates under light conditions (16 h at 100 $\mu\text{mol m}^{-2} \text{sec}^{-1}$) at 20°C. RNA was extracted from these samples using TRIzol[®] extraction (Invitrogen, Carlsbad, CA, USA) followed by two ethanol precipitations, then checked for RNA integrity with the Bioanalyzer from Agilent (Waldbronn, Germany). cRNAs were produced from 2 μg of total RNA from each pool with the 'Message Amp aRNA' kit (Ambion, Austin, TX, USA). Then 5 μg of cRNAs were reverse transcribed in the presence of 200 U of SuperScript II (Invitrogen), cy3-dUTP and

cy5-dUTP (NEN, Boston, MA, USA) according to Puskas *et al.* (2002) for each slide. Samples were combined, purified and concentrated with YM30 Microcon columns (Millipore). Slides were pre-hybridized for 1 h and hybridized overnight at 42°C in 25% formamide. Slides were washed in 2 \times SSC + 0.1% SDS (4 min), 1 \times SSC (4 min), 0.2 \times SSC (4 min), 0.05 \times SSC (1 min) and dried by centrifugation. Six hybridizations (three dye swaps) were carried out. The arrays were scanned on a GenePix 4000A scanner (Axon Instruments, Foster City, CA, USA) and images were analyzed by GenePix Pro 3.0 (Axon Instruments).

Statistical analysis of microarray data

The statistical analysis was performed as described in Lurin *et al.* (2004), based on two dye swaps, i.e. four arrays each containing the 24576 GSTs and 384 controls. The controls were used for assessing the quality of the hybridizations but were not included in the statistical tests. For each array, the raw data comprised the logarithm of the median feature pixel intensity at wavelength 635 nm (red) and 532 nm (green). No background was subtracted. In the following description, log-ratio refers to the differential expression between the mutant and the control. An array-by-array normalization was performed to remove systematic biases. Then we performed a global intensity-dependent normalization using the loess procedure (see Yang *et al.*, 2002) to correct the dye bias. Finally, on each block, the log-ratio median is subtracted from each value of the log-ratio of the block to correct a print-tip effect on each metablock. To determine differentially expressed genes, we performed a paired *t*-test on the log-ratios. The number of observations per spot varied between two and six and is inadequate for calculating a gene-specific variance. For this reason we assume that the variance of the log-ratios is the same for all genes. The raw *P*-values were adjusted by the Bonferroni method, which controls the family wise error rate (FWER).

Gene mapping

The F₂ mapping population was screened with SLP PCR-based markers designed by Bell and Ecker (1994). The primer sequences of the markers nga1139 and nga1107 were TTTTTCCTTGTTGCATTCC – TAGCCGGATGAGTTGGTACC and CGACGAATCGACAGAATTAGG – GCGAAAAACAAAAAATCCA, respectively.

DNA was extracted from cotyledons in a 96-well PCR plate as described for *cov1* mapping (Parker *et al.*, 2003). Cotyledons were ground on ice in 0.4 M NaOH. Seven microliters of extract were neutralized in 150 μl of 0.3 M cold Tris-HCl buffer (pH 8.0). The PCR was performed with Life Technology TAQ polymerase using a classic PCR program. The PCR products were run on 3% agarose gel to detect polymorphisms.

Acknowledgements

We are grateful to Patricia Nouvet and Carine Guiral for their technical assistance, Dr Catherine Perrot-Rechenmann for performing IAA transport experiments and Dr Karin Ljung for measurements of IAA content. We also thank Dr Catherine Digonnet for critically reading the manuscript. This work was supported by the Génoplatte Program, the Institut National de la Recherche Agronomique, the Centre National de la Recherche Scientifique and the Swedish Research Council. We thank the Nottingham Arabidopsis Stock Centre for providing seed stocks.

Supplementary Material

The following supplementary material is available for this article online:

Supplementary data S1. List of all differentially expressed genes in 10-day-old plantlets of *hca* as compared with wild type. Microarray analysis was performed using the CATMA (complete Arabidopsis transcriptome microarray). Genes are listed according to their log₂ ratio from the most upregulated to the most downregulated. For each gene, the locus name (At number), the CATMA number (Crowe *et al.*, 2003) and the putative ID are indicated. Note that the complete results of this experiment will soon be available on the Array Express website (<http://www.ebi.ac.uk/arrayexpress/>).

This material is available as part of the online article from <http://www.blackwell-synergy.com>

References

- Aida, M., Beis, D., Heidstra, R., Willemsen, V., Blilou, I., Galinha, C., Nussaume, L., Noh, Y.S., Amasino, R. and Scheres, B. (2004) The PLETHORA genes mediate patterning of the Arabidopsis root stem cell niche. *Cell*, **119**, 109–120.
- Aloni, R. (1995) The induction of vascular tissues by auxin and cytokinin. In *Plant Hormones: Physiology, Biochemistry and Molecular Biology* (Davies, P.J., ed.). Dordrecht: Kluwer Academic Publishers, pp. 531–546.
- Altamura, M.M., Possenti, M., Matteucci, A., Baima, S., Ruberti, I. and Morelli, G. (2001) Development of the vascular system in the inflorescence stem of *Arabidopsis*. *New Phytol.* **151**, 381–389.
- Åstot, C., Dolezal, K., Moritz, T. and Sandberg, G. (1998) Pre-column derivatization and capillary liquid chromatographic/frit-fast atom bombardment mass spectrometric analysis of cytokinins in *Arabidopsis thaliana*. *J. Mass Spectrom.* **33**, 892–902.
- Baima, S., Nobili, F., Sessa, G., Lucchetti, S., Ruberti, I. and Morelli, G. (1995) The expression of the *ATHB-8* homeobox gene is restricted to provascular cells in *Arabidopsis thaliana*. *Development*, **121**, 4171–4182.
- Baima, S., Possenti, M., Matteucci, A., Wisman, E., Altamura, M.M., Ruberti, I. and Morelli, G. (2001) The *Arabidopsis* ATHB-8 HD-zip protein acts as a differentiation-promoting transcription factor of the vascular meristems. *Plant Physiol.* **126**, 643–655.
- Bell, C.J. and Ecker, J.R. (1994) Assignment of 30 microsatellite loci to the linkage map of *Arabidopsis*. *Genomics*, **19**, 137–144.
- Berleth, T. and Jürgens, G. (1993) The role of the *MONOPTEROS* gene in organising the basal body region of the *Arabidopsis* embryo. *Development*, **118**, 575–587.
- Berleth, T. and Mattsson, J. (2000) Vascular development: tracing signals along veins. *Curr. Opin. Plant Biol.* **3**, 406–411.
- Berleth, T., Mattsson, J. and Hardtke, C.S. (2000) Vascular continuity and auxin signals. *Trends Plant Sci.* **5**, 387–393.
- Beschtoold, N., Ellis, J. and Pelletier, G. (1993) In planta *Agrobacterium*-mediated gene transfer by filtration of adult *Arabidopsis thaliana* plants. *C. R. Acad. Sci. (Paris)*, **316**, 1194–1199.
- Bonke, M., Thitamadee, S., Mahonen, A.P., Hauser, M.T. and Helariutta, Y. (2003) APL regulates vascular tissue identity in *Arabidopsis*. *Nature*, **426**, 181–186.
- Boyes, D.C., Zayed, A.M., Ascenzi, R., McCaskill, A.J., Hoffman, N.E., Davis, K.R. and Gorchach, J. (2001) Growth stage-based phenotypic analysis of *Arabidopsis*: a model for high throughput functional genomics in plants. *Plant Cell*, **13**, 1499–1510.
- Busse, J.S. and Evert, R.F. (1999) Vascular differentiation and transition in the seedling of *Arabidopsis thaliana* (Brassicaceae). *Int. J. Plant Sci.* **160**, 241–251.
- Carland, F.M. and McHale, N.A. (1996) *LOP1*: a gene involved in auxin transport and vascular patterning in *Arabidopsis*. *Development*, **122**, 1811–1819.
- Casson, S.A., Chilly, P.M., Topping, J.F., Evans, I.M., Souter, M.A. and Lindsey, K. (2002) The *POLARIS* gene of *Arabidopsis* encodes a predicted peptide required for correct root growth and leaf vascular patterning. *Plant Cell*, **14**, 1705–1721.
- Chaffey, N., Cholewa, E., Regan, S. and Sundberg, B. (2002) Secondary xylem Development in *Arabidopsis*: a model for wood formation. *Physiol. Plant.* **114**, 594–600.
- Chory, J., Reinecke, D., Sopheak Sim, S., Tracy Washburn, T. and Brenner, M. (1994) A role for cytokinins in de-etiolation in *Arabidopsis*, *det* mutants have an altered response to cytokinin. *Plant Physiol.* **104**, 339–347.
- Christensen, S.K., Dagenais, N., Chory, J. and Weigel, D. (2000) Regulation of auxin response by protein kinase PINOID. *Cell*, **100**, 469–478.
- Cluis, C.P., Mouchel, C.F. and Hardtke, C.S. (2004) The *Arabidopsis* transcription factor *HY5* integrates light and hormone signalling pathways. *Plant J.* **38**, 332–347.
- Coenen, C. and Lomax, T.L. (1997) Auxin–cytokinin interactions in higher plants: old problems and new tools. *Trends Plant Sci.* **2**, 351–356.
- Crowe, M.L., Serizet, C., Thareau, V. *et al.* (2003) CATMA: a complete Arabidopsis GST database. *Nucleic Acids Res.* **31**, 156–158.
- D'Agostino, I.B. and Kieber, J.J. (1999) Molecular mechanisms of cytokinin action. *Curr. Opin. Plant Biol.* **2**, 359–364.
- D'Agostino, I.B., Deruere, J. and Kieber, J.J. (2000) Characterization of the response of the *Arabidopsis* response regulator gene family to cytokinin. *Plant Physiol.* **124**, 1706–1717.
- Deikman, J. and Hammer, P.E. (1995) Induction of anthocyanin accumulation by cytokinins in *Arabidopsis thaliana*. *Plant Physiol.* **108**, 47–57.
- Edlund, A., Eklof, S., Sundberg, B., Moritz, T. and Sandberg, G. (1995) A microscale technique for gas chromatography-mass spectrometry measurements of picogram amounts of indole-3-acetic acid in plant tissues. *Plant Physiol.* **108**, 1043–1047.
- Esau, K. (1965) *Plant Anatomy*. New York, NY: John Wiley and Sons, Inc.
- Fukuda, H. (2004) Signals that control plant vascular cell differentiation. *Nature*, **5**, 379–391.
- Fukuda, H. and Komamine, A. (1980) Establishment of an experimental system for the study of tracheary element differentiation from single cells isolated from the mesophyll of *Zinnia elegans*. *Plant Physiol.* **65**, 57–60.
- Gälweiler, L., Guan, C., Müller, A., Wisman, E., Mendgen, K., Yephremov, A. and Palme, K. (1998) Regulation of polar auxin transport by AtPIN1 in *Arabidopsis* vascular tissue. *Science*, **282**, 2226–2230.
- Hardtke, C.S. and Berleth, T. (1998) The *Arabidopsis* gene *MONOPTEROS* encodes a transcription factor mediating embryo axis formation and vascular. *EMBO J.* **17**, 1405–1411.
- Hilson, P., Allemeersch, J., Altmann, T. *et al.* (2004) Versatile gene-specific sequence tags for Arabidopsis functional genomics: transcript profiling and reverse genetics applications. *Genome Res.* **14**, 2176–2189.
- Hobbie, L.J. (1998) Auxin: molecular and genetic approaches in *Arabidopsis*. *Plant Physiol. Biochem.* **36**, 91–102.
- Hobbie, L.J., Mc Govern, M., Hurwitz, L.R., Pierro, A., Liu, N.Y., Bandyopadhyay, A. and Estelle, M. (2000) The *axr6* mutants of *Arabidopsis thaliana* define a gene involved in auxin response and early development. *Development*, **127**, 23–32.
- Inoue, T., Higuchi, M., Hashimoto, Y., Seki, M., Kobayashi, M., Kato, T., Tabata, S., Shinozaki, K. and Kakimoto, T. (2001) Identification

- of CRE1 as a cytokinin receptor from *Arabidopsis*. *Nature*, **409**, 1060–1063.
- Jefferson, R.A., Kavanagh, T.A. and Bevan, M.W.** (1987) GUS fusions: beta-glucuronidase as a sensitive and versatile gene fusion marker in higher plants. *EMBO J.* **13**, 3901–3907.
- Jones, L., Ennos, A.R. and Turner, S.R.** (2001) Cloning and characterization of irregular xylem4 (*irx4*): a severely lignin-deficient mutant of *Arabidopsis*. *Plant J.* **26**, 205–216.
- Kiba, T., Yamada, H. and Mizuno, T.** (2002) Characterization of the ARR15 and ARR16 response regulators with special reference to the cytokinin signaling pathway mediated by the AHK4 histidine kinase in roots of *Arabidopsis thaliana*. *Plant Cell Physiol.* **43**, 1059–1066.
- Ko, J.H., Han, K.H., Park, S. and Yang, J.** (2004) Plant body weight-induced secondary growth in *Arabidopsis* and its transcription phenotype revealed by whole-transcriptome profiling. *Plant Physiol.* **135**, 1069–1083.
- Kubo, M. and Kakimoto, T.** (2000) Cytokinin-hypersensitive genes of *Arabidopsis* negatively regulate the cytokinin-signaling pathway for cell division and chloroplast development. *Plant J.* **23**, 385–394.
- Lachaud, S., Cateson, A.-M. and Bonnemain, J.-L.** (1999) Structure and functions of the vascular cambium. *C. R. Acad. Sci. (Paris)*, **322**, 633–650.
- Larson, P.R.** (1994) *The Vascular Cambium: Development and Structure*. Berlin: Springer-Verlag.
- Little, C.H.A. and Pharis, R.P.** (1995) Hormonal control of radial and longitudinal growth in the tree stem. In *Plant Stems. Physiology and Functional Morphology* (Gartner, B.L., ed.). Academic Press Publishers, pp. 281–319.
- Ljung, K., Hull, A.K., Kowalczyk, M., Marchant, A., Celenza, J., Cohen, J.D. and Sandberg, G.** (2002) Biosynthesis, conjugation, catabolism and homeostasis of indole-3-acetic acid in *Arabidopsis thaliana*. *Plant Mol. Biol.* **49**, 249–272.
- Lomax, T.L., Muday, G.K. and Ruberty, P.H.** (1995) Auxin transport. In *Plant Hormones: Physiology, Biochemistry and Molecular Biology* (Davies, P.J., ed.). Dordrecht: Kluwer Academic Publishers, pp. 509–530.
- Lurin, C., Andres, C., Aubourg, S. et al.** (2004) Genome-wide analysis of *Arabidopsis* pentatricopeptide repeat proteins reveals their essential role in organelle biogenesis. *Plant Cell*, **16**, 2089–2103.
- Mähönen, A.P., Bonke, M., Kauppinen, L., Riikonen, M., Benfey, P.N. and Helariutta, Y.** (2000) A novel two component hybrid molecule regulates vascular morphogenesis of the *Arabidopsis* root. *Genes Dev.* **14**, 2938–2943.
- Mok, D.W. and Mok, M.C.** (2001) Cytokinin metabolism and action. *Annu. Rev. Plant Physiol. Plant Mol. Biol.* **52**, 89–118.
- Nakano, J. and Meshitsuka, G.** (1992) The detection of lignin. In *Methods in Lignin Chemistry* (Dence, C.W. and Lin, S.Y., eds). New York: Springer-Verlag, pp. 23–61.
- Nordström, A., Tarkowski, P., Tarkowska, D., Norbaek, R., Astot, C., Dolezal, K. and Sandberg, G.** (2004) Auxin regulation of cytokinin biosynthesis in *Arabidopsis thaliana*: a factor of potential importance for auxin-cytokinin-regulated development. *Proc. Natl Acad. Sci. USA*, **101**, 8039–8044.
- Oh, S., Park, S. and Han, K.H.** (2003) Transcriptional regulation of secondary growth in *Arabidopsis thaliana*. *J. Exp. Bot.* **54**, 2709–2722.
- Oyama, T., Shimura, Y. and Okada, K.** (1997) The *Arabidopsis* HY5 gene encodes a bZIP protein that regulates stimulus-induced development of root and hypocotyl. *Genes Dev.* **11**, 2983–2995.
- Papi, M., Sabatini, S., Altamura, M.M., Hennig, L., Schafer, E., Costantino, P. and Vittorioso, P.** (2002) Inactivation of the phloem-specific Dof zinc finger gene DAG1 affects response to light and integrity of the testa of *Arabidopsis* seeds. *Plant Physiol.* **128**, 411–417.
- Parker, G., Schofield, R., Sundberg, B. and Turner, S.** (2003) Isolation of *COV1*, a gene involved in the regulation of vascular patterning in the stem of *Arabidopsis*. *Development*, **130**, 2139–2148.
- Ponce, M.R., Robles, P. and Micol, J.L.** (1999) High-throughput genetic mapping in *Arabidopsis thaliana*. *Mol. Gen. Genet.* **261**, 408–415.
- Puskas, L.G., Zvara, A., Hackler, L., Jr and Van Hummelen, P.** (2002) RNA amplification results in reproducible microarray data with slight ratio bias. *Biotechniques*, **32**, 1330–1334, 1336, 1338, 1340.
- Rashotte, A.M., Carson, S.D., To, J.P. and Kieber, J.J.** (2003) Expression profiling of cytokinin action in *Arabidopsis*. *Plant Physiol.* **132**, 1998–2011.
- Ratcliffe, O.J., Riechmann, J.L. and Zhang, J.Z.** (2000) INTERFASCICULAR FIBERLESS1 is the same gene as *REVOLUTA*. *Plant Cell*, **12**, 315–317.
- Sachs, T.** (1981) The control of the patterned differentiation of vascular tissues. *Adv. Bot. Res.* **9**, 152–262.
- Saks, Y., Feigenbaum, P. and Aloni, R.** (1984) Regulatory effect of cytokinin on secondary xylem fiber formation in an in vivo system. *Plant Physiol.* **76**, 638–648.
- Scarpella, E. and Meijer, A.H.** (2004) Pattern formation in the vascular system of monocot and dicot plant species. *New Phytol.* **164**, 209–242.
- Scarpella, E., Rueb, S. and Meijer, A.H.** (2003) The *RADICLELESS1* gene is required for vascular pattern formation in rice. *Development*, **130**, 645–658.
- Shibaoka, H.** (1994) Plant hormone-induced changes in the orientation of cortical microtubules: alterations in the cross-linking between microtubules and the plasma membrane. *Annu. Rev. Plant Physiol.* **45**, 527–544.
- Sieburth, L.E.** (1999) Auxin is required for leaf vein pattern in *Arabidopsis*. *Plant Physiol.* **121**, 1179–1190.
- Sundberg, B., Ugglä, C. and Tuominen, H.** (2001) Cambial growth and auxin gradients. In *Cell and Molecular Biology of Wood Formation* (Savidge, R.A., Barnett, J.R. and Napier, R., eds). Oxford, UK: BIOS Scientific Publishers Ltd, pp. 169–188.
- Swarup, R. and Bennett, M.** (2003) Auxin transport: the fountain of life in plants? *Dev. Cell*, **5**, 824–826.
- Taylor, N.G., Scheible, W.R., Cutler, S., Somerville, C.R. and Turner, S.R.** (1999) The irregular xylem 3 locus of *Arabidopsis* encodes a cellulose synthase required for secondary cell wall synthesis. *Plant Cell*, **11**, 769–779.
- To, J.P., Haberer, G., Ferreira, F.J., Deruere, J., Mason, M.G., Schaller, G.E., Alonso, J.M., Ecker, J.R. and Kieber, J.J.** (2004) Type-A *Arabidopsis* response regulators are partially redundant negative regulators of cytokinin signaling. *Plant Cell*, **16**, 658–671.
- Turner, S. and Sieburth, L.E.** (2002) Vascular patterning. In *The Arabidopsis Book* (Somerville, C.R. and Meyerowitz, E.M., eds). Rockville, MD: American Society of Plant Biologists, pp. 1–23.
- Ugglä, C., Moritz, T., Sandberg, G. and Sundberg, B.** (1996) Auxin as a positional signal in pattern formation in plants. *Proc. Natl Acad. Sci. USA*, **93**, 9282–9286.
- Wysocka-Diller, J.W., Helariutta, Y., Fukaki, H., Malamy, J.E. and Benfey, P.N.** (2000) Molecular analysis of SCARECROW function reveals a radial patterning mechanism common to root and shoot. *Development*, **127**, 595–603.
- Yang, Y.H., Dudoit, S., Luu, P., Lin, D.M., Peng, V., Ngai, J. and Speed, T.P.** (2002) Normalization for cDNA microarray data: a

- robust composite method addressing single and multiple slide systematic variation. *Nucleic Acids Res.* **30**, 15.
- Ye, Z.H.** (2002) Vascular tissue differentiation and pattern formation in plants. *Annu. Rev. Plant Biol.* **53**, 183–202.
- Ye, Z.H., Freshour, G., Hahn, M.G., Burk, D.H. and Zhong, R.** (2002) Vascular development in *Arabidopsis*. *Int. Rev. Cytol.* **220**, 225–256.
- Zhao, C., Johnson, B.J., Kositsup, B. and Beers, E.P.** (2000) Exploiting secondary growth in *Arabidopsis*. Construction of xylem and bark cDNA libraries and cloning of three xylem endopeptidases. *Plant Physiol.* **123**, 1185–1196.
- Zhong, R. and Ye, Z.** (1999) *IFL1* a gene regulating interfascicular fiber differentiation in *Arabidopsis*, encodes a homeodomain-leucine zipper protein. *Plant Cell*, **11**, 2139–2152.
- Zhong, R., Taylor, J.J. and Ye, Z.** (1997) Disruption of interfascicular fiber differentiation in an *Arabidopsis* mutant. *Plant Cell*, **9**, 2159–2170.